
<https://doi.org/10.15407/ujpe69.5.293>

A.YU. OVCHARENKO, O.A. LEBED'

Institute of Applied Physics, Nat. Acad. of Sci. of Ukraine
(58, Petropavlivska Str., Sumy 40030, Ukraine; e-mail: oartturr@gmail.com)

DETECTION OF STRUCTURAL FEATURES OF OBJECTS USING X-RAY PHASE-CONTRAST IMAGING METHOD

Phase contrast is widely used everywhere, where the visualization of the internal structure of objects using X-rays is required. In this paper, a new approach based on the Fresnel–Kirchhoff theory has been proposed to model the X-ray phase-contrast image making use of the free-propagation method. A simple calculation model has been developed that allows the intensity variation on three-dimensional models of macroscopic objects with arbitrary shapes and, accordingly, the observation conditions for obtaining a contrast image in the case of known detector system characteristics and X-ray source intensity to be determined. The possibility of obtaining the clear images of objects with low refractive indices and determining their geometric dimensions and thickness is shown. The approaches described in this paper can be useful for developers of compact devices aimed at detecting structural inhomogeneities inside the studied objects with the help of non-destructive methods.

Keywords: X-ray phase-contrast imaging, wave front, X-ray diffraction, coherence, Fresnel–Kirchhoff diffraction theory.

1. Introduction

Control over the quality and reliability of modern materials and products is an extremely challenging task in many branches of industry and scientific research. It is of special importance in the energy, transport, and medical fields, where a product failure can lead to man-made disasters and human casualties. Complicated technical objects often possess internal defects and hidden structural inhomogeneities that cannot be detected by conventional control methods and substantially reduce the reliability and service life of those constructions.

Citation: Ovcharenko A., Lebed O. Detection of structural features of objects using X-ray phase contrast imaging method. *Ukr. J. Phys.* **69**, No. 5, 293 (2024). <https://doi.org/10.15407/ujpe69.5.293>.

Цитування: Овчаренко А.Ю., Лебедь О.А. Виявлення структурних особливостей об'єктів методом рентгенівського фазового контрасту. *Укр. фіз. журн.* **69**, №5, 293 (2024).

ISSN 2071-0194. Ukr. J. Phys. 2024. Vol. 69, No. 5

At the same time, X-ray radiation (XR) serves as an important diagnostic tool in biology and medicine. Most of the traditional methods of medical and industrial radiography, tomography, and microscopy are usually based on a change in the X-ray absorption coefficient in different parts of the object due to changes in the object's density, composition, and thickness. The application of hard XR in tomography makes it possible to prevent its complete absorption and obtain information about the internal structure of larger objects by means of a non-destructive method. From whence, it follows that, in order to reduce the radiation dose, it is necessary to develop methods based on the X-ray refraction phenomenon. Therefore, the development of principally new approaches to non-destructive testing is a key task for scientific and technical progress and the development of medicine.

One of the most promising methods in this domain is the X-ray phase tomography, which is based on

the analysis of the spatial distribution of the phase of coherent radiation that passes through examined object. Unlike ordinary radiography, this method has a much higher sensitivity to internal inhomogeneities of the material at the micron and submicron levels; in particular, these are microcracks, pores, and so forth. Therefore, the X-ray phase tomography has been successfully used recently in the aerospace industry and mechanical engineering while making a rapid analysis of products and structures [1, 2]. It also becomes a more and more applied tool of the medical visualization owing to the high contrast of soft tissues [3].

X-rays possess a high penetration ability into most materials, so they can be used to study the internal structure of an object without destroying the latter. Currently, traditional methods are based on the difference between the ability of different areas in the researched object to absorb X-rays because of changes in the object's density, composition, and thickness. This task becomes considerably complicated when studying weakly absorbing objects, for example, soft biological tissues. Although X-rays can penetrate deeply into such materials, the contrast of the corresponding images is weak due to the smallness of the absorption coefficient gradient.

The studies of relatively large biological objects using the methods based on the absorption phenomenon require the application of hard radiation, the introduction of contrast agents, and, accordingly, larger radiation doses. The X-ray phase-contrast (XPC) method allows the visualization of the internal structure of weakly absorbing objects to be performed with a high spatial resolution, even if the substance density gradients are small. This method is based on the phenomenon of X-ray refraction in the object, which leads to variations in the wave phase front [3–10]. As a result of such phase changes, X-rays deviate from their initial directions at small angles whose values depend on the spatial distribution of the substance density in the examined object. From the viewpoint of wave optics, the phase-contrast images are a result of the interference between the incident wave and the waves that have passed through the specimen. The study of objects using the methods based on the X-ray refraction phenomenon is a challenging task for many areas of modern applied science and medicine.

Contrast X-ray radiation images are considered to be promising technologies in medicine, which can en-

hance the contrast resolution of radiographic methods [3, 8]. This technology will allow the functioning of installations of standard X-ray computed tomography diagnostics and scanning nuclear magnetic resonance systems. In the future, the application of XPC methods for early diagnosis and medical imaging will allow the solution of the main problems in this direction: the reduction of the radiation dose and the enhancement of the resolution and contrast at the visualization of soft tissues at the early stages of diseases.

In this paper, the propagation-based phase-contrast method, since it is one of the most widespread methods used for obtaining phase-contrast images. A similar scheme was applied for the first time by Gabor in an electron microscope experiment [11] and was later developed as a phase-diversity method in the X-ray spectral interval [5, 12–18]. An important advantage of this method is the simplicity of its experimental implementation, which does not require the usage of complicated X-ray optical elements.

However, the comprehensive and effective application of this method in practice requires substantial improvements in both the hardware and the physical-mathematical models that are used to describe the process of phase contrast formation. In particular, urgent is the problem of creating compact phase tomography installations via the optimization of their design parameters and operating modes by means of simulating the corresponding physical processes. Nowadays, this issue attracts insufficient attention, so there arise several situational problems that need to be solved.

2. Analytical Model of Free-Propagation Method

The free-propagation method (or the linear phase-contrast method) is implemented in the region of Fresnel diffraction [3–6, 18–23]. Internal variations in the thickness and the XR refractive index of the researched object lead to changes in the X-ray wavefront shape, when this front passes through the object. If a detector is arranged directly behind the examined object, we obtain an ordinary X-ray absorption image. But if the distance from the object to the detector is substantial, an X-ray phase-contrast image is formed. The optical properties of the experimental object can be characterized by the complex refractive

index

$$n = 1 - \delta + i\beta, \quad (1)$$

where the dimensionless quantity β describes the absorption properties of the material under study (the absorption index), and the dimensionless quantity δ describes the phase shift of the wavefront associated with the passage of the rays through the object. The phase shift of the X-wave that has passed through the specimen depends on the variations of the refractive decrement in the specimen, as well as the specimen's thickness. In the case of a monochromatic parallel beam that propagates along the z -axis, the phase variation can be written in the following form:

$$\varphi(x, y) = -\frac{2\pi}{\lambda} \int \delta(x, y, z) dz, \quad (2)$$

where the integral is calculated over the entire thickness of the object in the direction of XR propagation.

In this work, to calculate phase-contrast images, we took the Fresnel–Kirchhoff scalar diffraction theory as a basis for the calculation model. This model allows the wave front evolution to be taken into account along both the paths “source–object” and “object–screen”.

In Fig. 1, a schematic diagram is shown for the path of rays propagating from the X-ray source through the examined object to the screen. This approach is quite general and is suitable for calculating diffraction patterns generated by both point and extended radiation sources. In addition, it is possible to perform a numerical experiment for objects of any geometric shape and with sizes ranging from the mesoscopic scale to the macroscopic one.

In the case of an X-ray beam propagating from a point source, the expression for the radiation intensity in the detector plane can be written in the form [18, 24]

$$\psi(x_{scr}, y_{scr}) = \frac{1}{i\lambda} \int_{-\infty}^{\infty} \int_{-\infty}^{\infty} \sqrt{I_0} \frac{\exp(ik(r+s))}{rs} \times \left[\frac{\cos(\mathbf{n}, \mathbf{r}) + \cos(\mathbf{n}, \mathbf{s})}{2} \right] \exp(i\varphi) dx_{obj} dy_{obj}, \quad (3)$$

where

$$s = \sqrt{(x_{obj} - x_{source})^2 + (y_{obj} - y_{source})^2 + R^2}; \quad (4)$$

$$r = \sqrt{(x_{obj} - x_{scr})^2 + (y_{obj} - y_{scr})^2 + \Delta^2};$$

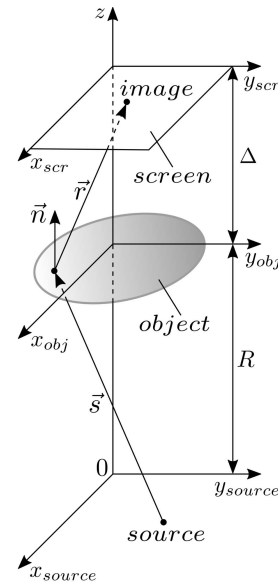


Fig. 1. General schematic diagram for the calculation of the phase-contrast image in the framework of the Fresnel–Kirchhoff diffraction theory

\mathbf{s} and \mathbf{r} are the “source–object” and “object–screen” vectors, respectively; λ is the radiation wavelength; \mathbf{n} is the normal to the object plane; and φ is an additional phase shift induced by the impact of the object on the incoming wavefront.

3. Research Methodology

Nowadays, there are a very small number of works on the computer simulation of X-ray diffraction at various objects. In our opinion, this fact can be explained by several reasons. First, a simulation of this kind requires the availability of sufficiently powerful computing resources, because the correct calculation of integral (3) can be carried out only numerically, by splitting the object and screen planes into a very large number of points and using the double precision, when calculating all quantities entering this formula. In turn, this leads to problems associated with the processing of experimental data in the real-time mode. Second, although the above-mentioned model is quite universal and does not contain restrictions on the size and geometric shape of studied objects, it is rather difficult to model three-dimensional objects with irregular geometric shapes. In this regard, the simulation is carried out, as a rule, for very simple objects and assuming that their dimensions are

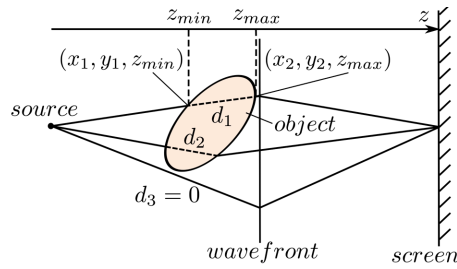


Fig. 2. Schematic diagram for the calculation of the specimen thickness and the X-ray phase shifts

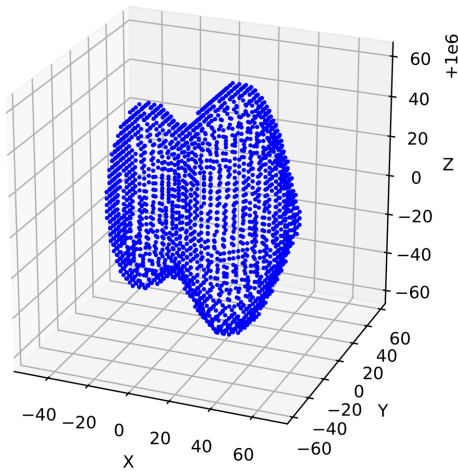


Fig. 3. An examined object with a maximum linear size of about 100 μm

much smaller than the distance from the source to the object and are characterized by a certain symmetry. The thickness of the objects was simply given analytically, which is a considerable limitation when performing studies of this kind.

The application of the Fresnel–Kirchhoff scalar theory of diffraction allowed us to develop an approach for the simulation of X-ray diffraction at the models of real three-dimensional objects with arbitrary geometric shapes. Figure 2 illustrates the calculation scheme for the thicknesses of researched objects and the phase shifts of X-ray waves, which was implemented in our work. For this purpose, the examined three-dimensional object was defined as the geometric loci of points that formed the object’s surface. Then the object plane was split into a large number of points, and each of them was connected by a straight line with the radiation source. Using the equation of this straight line and the coordinates of

the object points, the intersection points (x_1, y_1, z_{\min}) and (x_2, y_2, z_{\max}) were determined, and the object thickness

$$d_1 = \sqrt{(x_2 - x_1)^2 + (y_2 - y_1)^2 + (z_{\max} - z_{\min})^2}$$

and the phase shift $\varphi = k\delta d_1$, where δ is the index of refraction, were calculated.

4. Results and Their Discussion

The presented study is a part of works dealing with the planning and performing of experiments on the X-ray phase contrast using the free-propagation method and executing at the Associated International Laboratory LIA/IRP IDEATE [25, 26].

A point source with the wavelength $\lambda = 1.5 \times 10^{-4} \mu\text{m}$ was considered, which corresponded to the characteristic line $\text{CuK}\alpha$. As a studied specimen, the object shown in Fig. 3 was chosen. Its maximum geometric dimensions were selected to equal 100, 80, and 120 μm along the x -, y -, and z -axes, respectively, which allows the specimen size to be classified as macroscopic. For obtaining a phase-contrast image of the examined specimen, the distance from the radiation source to the center of the object was put $R = 1 \text{ m}$, and the distance from the center of the object to the screen $\Delta = 2.7 \text{ m}$. The numbers of points at the object and screen planes were equal to 845650 and 320400, respectively. Although such a splitting is minimalistic, it allowed us to obtain a rather high-quality image of the object. At the same time, it required the calculation of about 10^{12} parameters, according to formula (3).

Figure 4 demonstrates the image of the specimen (panel *a*) and the spatial signal of the object for an angle of 0 (panel *b*) in the xy -plane. The figure allows one to see the contours of the object, when the latter is observed along the z -axis and estimate the specimen dimensions along the x - and y -axes.

Indeed, if we take into account that the zoom factor M is equal to

$$M = 1 + \frac{\Delta}{R} = 3.7 \tag{5}$$

in our case and determine the maximum size of the object from the plot in Fig. 4, *b* as the distance between the points, where the perceptible oscillations in the central part of the plot begin and end (this is the region, where the specimen is located), then the

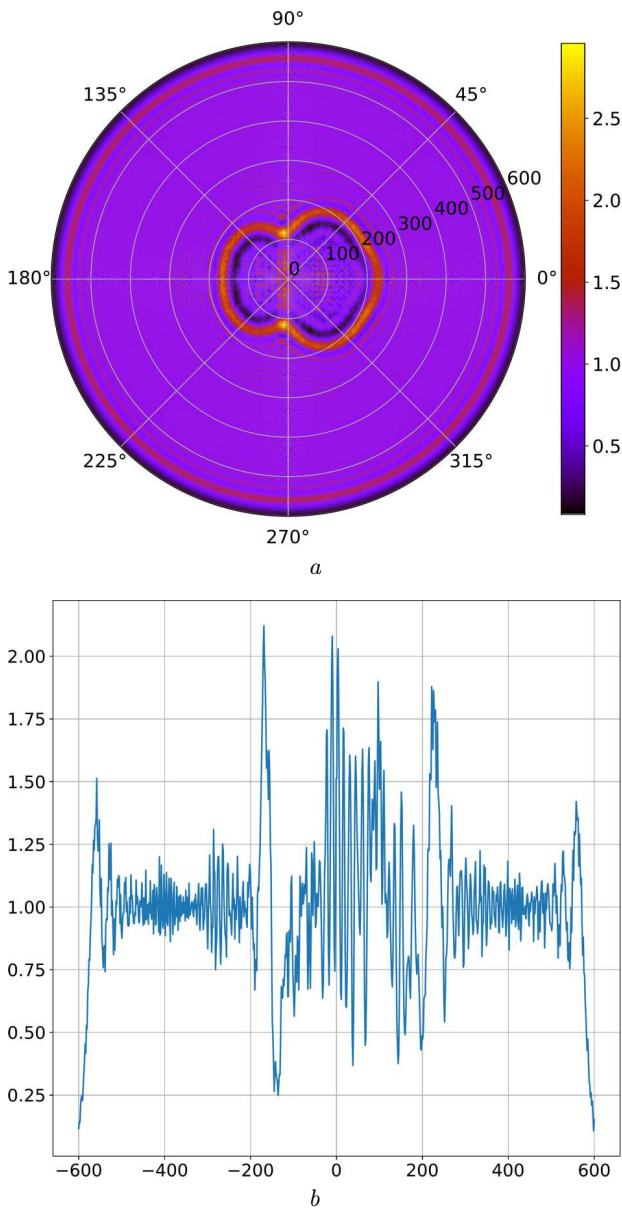


Fig. 4. The specimen image in the xy -plane (a) and the profile of the object signal (b)

following results are obtained. The oscillations start approximately at the point $x_1 = -180 \mu\text{m}$ and terminate at the point $x = 220 \mu\text{m}$. This means that the maximum image size of the studied object along the x -axis is approximately equal to $400 \mu\text{m}$. Therefore, taking the zoom factor value into account [see formula 5], the real size of the object along the x -axis is approximately equal to $108 \mu\text{m}$. We may assume that

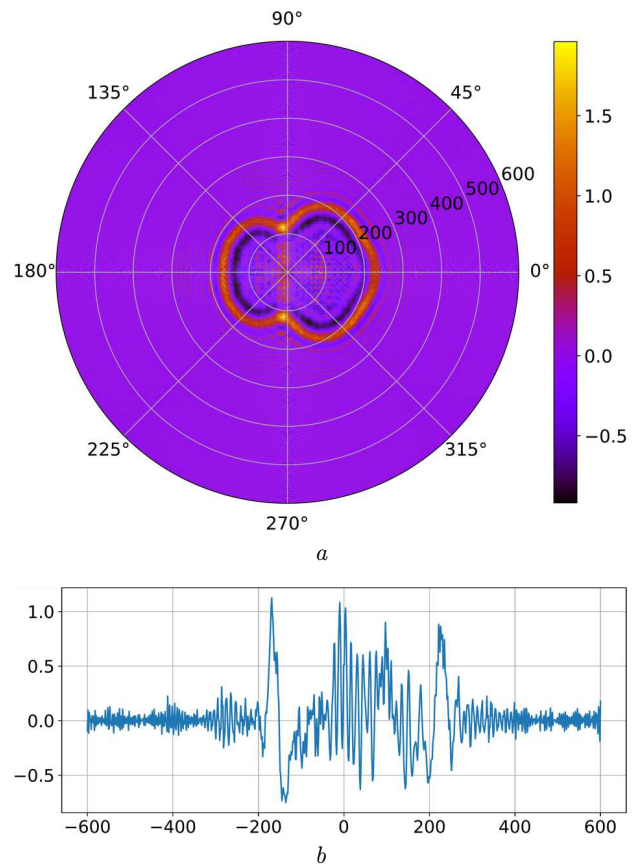


Fig. 5. The image of the object after cleaning from aperture diffraction (a) and the relative profile of the object signal (b)

this result of approximate calculation is completely consistent with the real size of the simulated object ($100 \mu\text{m}$ along the x -axis).

As concerning information about the thickness of the researched specimen along the XR propagation direction, we cannot obtain it directly from the data presented in Fig. 4. To solve this problem, it is necessary to construct the image of the specimen and the spatial signal of the object using the relative signal intensity (the difference between the signals obtained with and without the specimen) as is shown in Fig. 5. This procedure makes it possible to get rid of the influence of diffraction maxima and minima obtained from the aperture edges, reduces the oscillations, and allows the contours of the examined object to be determined more accurately.

In our research, we took a specimen with the low refractive index $\delta = 10^{-6}$, which corresponds to biological objects. To obtain more accurate information

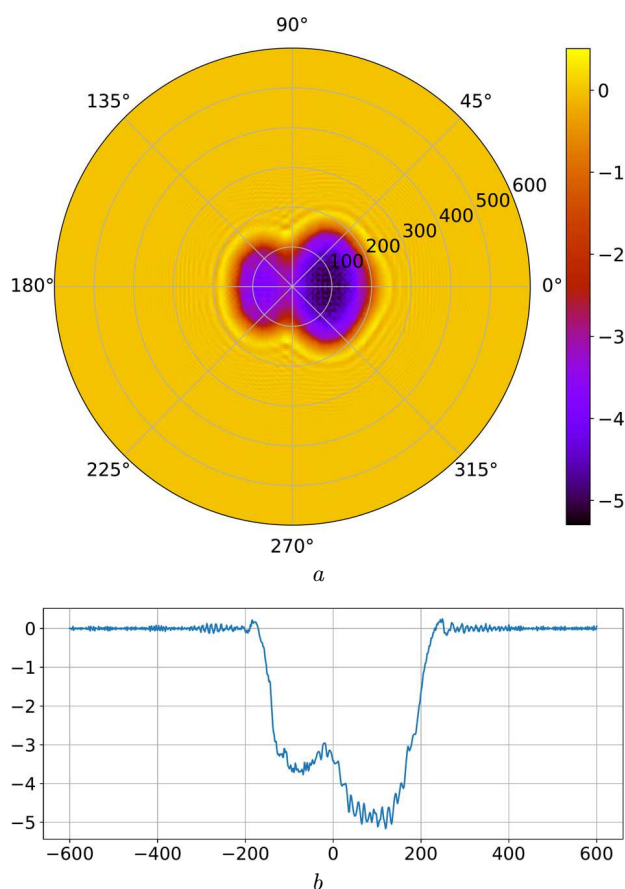


Fig. 6. Phase image of the object (a) and its phase profile (b)

about the geometric shape and thickness of the object, we calculated the phase profile and constructed a corresponding image (Fig. 6). The obtained result testifies that our simulation parameters for X-ray diffraction at the selected specimen were correct.

On the basis of the calculated complex amplitudes of previous images (obtained with and without the object), the X-ray phase value was found for each case, and their difference was determined. In this way, we calculated the spatial distribution of the X-ray phase shift induced by the object. It should be noted that detectors can register only the intensity but not the phase of X-ray radiation. That is why the combination of data on the radiation intensity and phase gives more complete information about the researched objects. By comparing the image intensity data for various areas and the phase profile plot with the geometric shape of the specimen (Fig. 3), a complete correspondence can be seen.

5. Conclusions

In this work, a new approach has been proposed to simulate X-ray diffraction at three-dimensional models of macroscopic objects with arbitrary shapes, which allows the thickness of the examined specimens to be calculated more accurately in comparison with the results obtained by other authors. The method of X-ray phase contrast imaging was applied to demonstrate the possibility of obtaining clear images of objects with low refractive indices and determining their geometric dimensions and thicknesses. The approaches presented in this work can be useful for the developers of compact devices aimed at detecting structural inhomogeneities in the studied objects making use of non-destructive methods.

The work was sponsored in the framework of the state research project No. 0122U000417 and the Associated International Laboratory LIA/IRP IDEATE.

1. M. Endrizzi. X-ray phase-contrast imaging. *Nucl. Instrum. Methods A* **878**, 88 (2018).
2. Y.S. Kashyap, P.S. Yadav, T. Roy, P.S. Sarkar, M. Shukla, A. Sinha. Laboratory-based X-ray phase-contrast imaging technique for material and medical science applications. *Appl. Radiat. Isot.* **66**, 1083 (2008).
3. A. Bravin, P. Coan, P. Suortti. X-ray phase-contrast imaging: from pre-clinical applications towards clinics. *Phys. Med. Biol.* **58**, R1 (2012).
4. T. Tuohimaa, M. Otendal, H.M. Hertz. Phase-contrast x-ray imaging with a liquid-metal-jet-anode microfocus source. *Appl. Phys. Lett.* **91**, 074104 (2007).
5. A. Snigirev, I. Snigireva, V. Kohn, S. Kuznetsov, I. Schelokov. On the possibilities of x-ray phase contrast microimaging by coherent high-energy synchrotron radiation. *Rev. Sci. Instrum.* **66**, 5486 (1995).
6. K.A. Nugent, T.E. Gureyev, D.F. Cookson, D. Paganin, Z. Barnea. Quantitative phase imaging using hard X-rays. *Phys. Rev. Lett.* **77**, 2961 (1996).
7. R.A. Lewis. Medical phase contrast x-ray imaging: Current status and future prospects. *Phys. Med. Biol.* **49**, 3573 (2004).
8. F. Arfelli, M. Assante, V. Bonvicini, A. Bravin, G. Cantatore, E. Castelli, L.D. Palma, M.D. Michiel, R. Longo, A. Olivo, S. Pani, D. Pontoni, P. Poropat, M. Prest, A. Rashevsky *et al.* Low-dose phase contrast X-ray medical imaging. *Phys. Med. Biol.* **43**, 2845 (1998).
9. S. Tao, C. He, X. Hao, C. Kuang, X. Liu. Principles of different X-ray phase-contrast imaging: A Review. *Appl. Sci.* **11**, 2971 (2021).
10. A. Momose. X-ray phase imaging reaching clinical uses. *Phys. Medica* **79**, 93 (2020).

11. D. Gabor. A new microscopic principle. *Nature* **161**, 777 (1948).
12. S.W. Wilkins, T.E. Gureyev, D. Gao, A. Pogany, A.W. Stevenson, Phase-contrast imaging using polychromatic hard X-rays. *Nature* **384**, 335 (1996).
13. A. Pogany, D. Gao, S.W. Wilkins. Contrast and resolution in imaging with a microfocus X-ray source. *Rev. Sci. Instrum.* **68**, 2774 (1997).
14. A. Peterzol, A. Olivo, L. Rigon, S. Pani, D. Dreossi. The effects of the imaging system on the validity limits of the ray-optical approach to phase contrast imaging. *Med. Phys.* **32**, 3617 (2005).
15. A. Burvall, U. Lundstrom, P. Takman, D. Larsson, H. Hertz. Phase retrieval in X-ray phase-contrast imaging suitable for tomography. *Opt. Express* **19**, 10359 (2011).
16. S.C. Mayo, A.W. Stevenson, S.W. Wilkins. In-line phase-contrast X-ray imaging and tomography for materials science. *Materials* **5**, 937 (2012).
17. A.J. Carroll, G.A. van Riessen, E. Balaur, I.P. Dolbnya, G.N. Tran, A.G. Peele. An iterative method for near-field Fresnel region polychromatic phase contrast imaging. *J. Opt.* **19**, 075003 (2017).
18. D. Paganin. *Coherent X-Ray Optics* (Oxford University Press, 2013).
19. D.M. Paganin, D. Pelliccia. Tutorials on x-ray phase contrast imaging: Some fundamentals and some conjectures on future developments, arXiv:1902.00364.
20. D. Paganin, S.C. Mayo, T.E. Gureyev, P.R. Miller, S.W. Wilkins. Simultaneous phase and amplitude extraction from a single defocused image of a homogeneous object. *J. Microsc.* **206**, 33 (2002).
21. S.W. Wilkins, T.E. Gureyev, D. Gao, A. Pogany, A.W. Stevenson. Phase-contrast imaging using polychromatic hard X-rays, *Nature* **384**, 335 (1996).
22. D. Paganin, K.A. Nugent. Noninterferometric phase imaging with partially coherent light. *Phys. Rev. Lett.* **80**, 2586 (1998).
23. P.C. Diemoz, A. Bravin, P. Coan. Theoretical comparison of three X-ray phase-contrast imaging techniques: Propagation-based imaging, analyzer-based imaging and grating interferometry. *Opt. Express* **20**, 2789 (2012).
24. A. Olivo, E. Castelli. X-ray phase contrast imaging: From synchrotrons to conventional sources, *Riv. Nuovo Cimento* **37**, 467 (2014).
25. O.M. Buhay, A.A. Drozdenko, M.I. Zakharets, I.G. Ignat'ev, A.B. Kramchenkov, V.I. Miroshnichenko, A.G. Ponomarev, V.E. Storizhko. Current status of the IAP NASU accelerator-based analytical facility. *Phys. Procedia* **66**, 166 (2015).
26. K. Dupraz *et al.* The ThomX ICS source. *Physics Open* **5**, 100051 (2020).

Received 23.02.24.

Translated from Ukrainian by O.I. Voitenko

А.Ю. Овчаренко, О.А. Лебедь

ВИЯВЛЕННЯ СТРУКТУРНИХ ОСОБЛИВОСТЕЙ ОБ'ЄКТІВ МЕТОДОМ РЕНТГЕНІВСЬКОГО ФАЗОВОГО КОНТРАСТУ

Фазовий контраст знаходить широке застосування в усіх галузях, де потрібна візуалізація внутрішньої структури об'єктів за допомогою рентгенівського випромінювання. У роботі запропоновано новий підхід моделювання фазоконтрастного рентгенівського зображення методом вільного поширення на основі теорії Френеля–Кірхгофа. Розроблена проста розрахункова модель дозволяє визначити значення зміни інтенсивності на тривимірних моделях об'єктів макроскопічних розмірів довільної форми і, відповідно, умови спостереження контрастного зображення при відомих характеристиках детекторної системи та інтенсивності джерела випромінювання. Була показана можливість одержання чітких зображень об'єктів з малими показниками заломлення, визначення їх геометричних розмірів та товщини. Викладені у роботі підходи можуть бути корисні розробникам компактних пристроїв для виявлення структурних неоднорідностей всередині досліджуваних об'єктів неруйнівним методом.

Ключові слова: рентгенівський фазовий контраст, хвильовий фронт, дифракція рентгенівського випромінювання, когерентність, теорія дифракції Френеля–Кірхгофа.